JOURNAL OF SOLID STATE CHEMISTRY 119, 90–97 (1995)

A Reinvestigation of the Preparation of Tungsten Oxide Hydrate WO_3, $1/3H_2O$

J. Pfeifer,[1] Cao Guifang,[2] P. Tekula-Buxbaum, B. A. Kiss, M. Farkas-Jahnke, and K. Vadasdi

Research Institute for Technical Physics of the Hungarian Academy of Sciences, H-1047 Budapest, Fóti út 56, P.O.B. 76, H-1325 Budapest, Hungary

Received December 30, 1994; in revised form April 3, 1995; accepted April 5, 1995

A reinvestigation of the synthesis procedures of WO_3, $1/3H_2O$ via the preparation and dehydration of H_2WO_4, H_2O has been carried out in order to check the stoichiometry of WO_3, $1/3H_2O$, the parent material of the important hexagonal WO_3. The formation of WO_3, $1/3H_2O$ during dehydration reaction of H_2WO_4, H_2O via the solution was observed to require the presence of sodium in the reaction system, resulting in sodium incorporation in the WO_3, $1/3H_2O$ phase. The minimal level of sodium in the WO_3, $1/3H_2O$ phase was found to be 160 ppm; sodium levels up to 1000–3000 ppm were also found to be incorporated in the WO_3, $1/3H_2O$ structures. A shift in the c parameter of the WO_3, $1/3H_2O$ cell has been found to be connected with the change in the concentration of incorporated sodium. The average size of the octagonal platelets of WO_3, $1/3H_2O$ was found to be connected with the sodium concentration in the solid phase. A modification in infrared absorption spectra has been observed.

INTRODUCTION

In recent years several works have been published on a metastable form of tungsten trioxide with a hexagonal structure (1–7). References (1, 2, 4, 6, and 7) consider the same hexagonal WO_3 matrix with a WO_3 stoichiometric composition. The open hexagonal WO_3 is the starting material for certain applications (2, 7, 8) and its structure is the basis of computer simulation studies for better understanding the hexagonal tungsten bronze structures (9). The proposed preparation route of h-WO_3 (1) consists of two steps. In the first step tungsten oxide hydrate, WO_3, $1/3H_2O$, is prepared from sodium tungstate, Na_2WO_4. In the second step h-WO_3 is prepared by dehydration of the precursor hydrate WO_3, $1/3H_2O$. The first step, the preparation of WO_3, $1/3H_2O$ (4), begins with the precipitation of tungstic acid gel (H_2WO_4, H_2O) from acidified Na_2WO_4 solution. After a successive washing procedure the precipitate, H_2WO_4, H_2O, is put into an autoclave and during a hydrothermal process a partial dehydration of H_2WO_4, H_2O results in WO_3, $1/3H_2O$. The structural filiation between the precursor WO_3, $1/3H_2O$ and hexagonal WO_3 gives importance to the synthesis procedures (involving the elimination of sodium) and the resulting structure of tungsten oxide hydrates H_2WO_4, H_2O and WO_3, $1/3H_2O$. The structure of WO_3, $1/3H_2O$ was determined by the X-ray powder diffraction method (4). Problems concerning the state and location of water in the mean WO_3, $1/3H_2O$ structure have already been revealed in Refs. (4 and 10). This study is concerned with the method of preparation and the crystallographic and morphological characteristics of WO_3, $1/3H_2O$ as regards residual or deliberately added sodium. The necessity of a more elaborate model of WO_3, $1/3H_2O$, which has the same WO_3, $1/3H_2O$ matrix but takes into account the presence of residual sodium, is pointed out in this paper.

EXPERIMENTAL DETAILS

Preparation of Tungstic Acid Samples

Tungstic acid samples were prepared according to Zocher's method (11), which was also employed in Ref. (4), for the preparation of WO_3, $1/3H_2O$.

Ten and a half grams of Na_2WO_4, $2H_2O$ of analytical grade (from Reanal, Hungary) was dissolved in 150 ml of water and the solution was cooled to 5°C. To this, 75 ml of normal hydrochloric acid solution (analytical grade, 18% in excess of equimolar reaction) cooled to the same temperature was added in several doses (to keep reaction temperature not higher than 5°C). The mixture was stirred for 1.5 hr in an ice bath and for 0.5 hr at room temperature. After leaving it for about 5 min, then centrifuging (5000 r.p.m., 3 min), the supernatant liquid was removed. Then 600 ml of water was added to the precipitate and the suspension was stirred 10 to 15 min in order to ensure the thorough assimilation of the gel. The steps of centrifuging, removing the supernatant liquid, and adding 600 ml of

[1] To whom correspondence should be addressed.

[2] Permanent address: Central South University of Technology, Changsha, Hunan, P. R. China.

0022-4596/95 $12.00

new water were repeated three to seven times. Intervals between washing steps ranged from 1 to 20 hr. At the end of the washing the pH value of the supernatant liquid varied between 3 and 4.5, corresponding to the number of washing steps. Throughout the experiments properly cleaned polythene or Teflon laboratory vessels and tools and deionized water (2 μS cm^{-1}) of a <0.1–0.2 ppm sodium level were used.

Dehydration of H_2WO_4, H_2O

The dehydration of H_2WO_4, H_2O was done according to Ref. (4). After the last centrifuging the precipitates were dispersed in 1000 ml of water and the suspensions were heated for 20 hr at 120°C in a stirred (200 r.p.m.) autoclave (Parr Instruments, Model 4552), under an atmosphere of 80% nitrogen +20% oxygen; the pressure before heating was 10 bar.

Samples were also prepared by deliberate Na addition. Several portions of precipitates washed seven times were homogenized and then distributed into parts. One of the portions was treated as described above. To the other samples various amounts of Na_2WO_4, $2H_2O$ were added before they were put into the autoclave for a similar treatment.

Determination of Sodium Content

Sodium content was determined in the dehydrated samples from the autoclave, in the precursor tungstic acid precipitates, and in the rinsing waters (removed supernatant liquids) throughout the washing process. Atomic absorption spectrophotometry (Perkin–Elmer 5000 Atomic Absorption Spectrophotometer, flame technique) was chosen as a suitable method for direct determination of small amounts of sodium in the presence of tungsten (12). The reagents used were of Suprapur grade from Merck with low residual sodium content: hydrochloric acid (30% HCl), max. 0.5 ppm; hydrogen peroxide (30% H_2O_2), max. 0.1 ppm; ammonia solution (25% NH_4OH), max. 0.05 ppm; potassium hydroxide (KOH, H_2O), max. 5 ppm; and caesium chloride (CsCl), max. 5 ppm. The range of the atomic absorption measurements was 0.1 to 1.5 μg sodium/ml, achieved by suitable weighing in and/or using a multiple-stage dilution technique; the error of the determination varied between 5 and 10%.

The procedures of the chemical analysis were as follows. Test solutions of rinsing waters were prepared by adding diluted HCl and H_2O_2 (for keeping the tungstic acid in solution) and CsCl solution (as Cs ionization buffer) and were diluted to a suitable volume. Precipitates, freshly prepared and dried at room temperature, were generally dissolved in ammonia solution and their test solutions were prepared using Cs ionization buffer. Crystalline samples after the treatment in the autoclave cannot be dissolved in ammonia solution. These samples were fused with KOH in a silver dish and then dissolved with water, producing test solutions with K as ionization buffer. Test solutions from freshly precipitated samples were also made by fusing with KOH for comparison.

Characterization

X-ray powder patterns were recorded at room temperature in a Guinier focusing camera using Cu$K\alpha$ radiation (λ = 0.154051 nm). The positions of the lines on the film were determined either visually or by computer-controlled densitometric analysis (13). Lattice parameters were obtained from the least-squares refinement of the d values of 23–26 reflections in the range $13° < 2\Theta < 30°$. For the determination of the total water contained in the samples, thermogravimetric analysis (Mettler, Registrierender Vakuum-Thermoanalyzer) was applied. Dehydration of WO_3, $1/3H_2O$ under a nitrogen–oxygen (80–20%) atmosphere by an isotherm treatment at about 300°C was carried out, to check the structure of the obtained WO_3. Infrared absorption spectra were taken by SPECORD 75 IR equipment in the range 400–4000 cm^{-1}, and by a Perkin–Elmer 783 IR spectrophotometer in the range 250–500 cm^{-1}; 2 mg sample/1 g KBr pellets was used. Crystallite habit and grain size distribution were studied by scanning electron microscopy with a JEOL 25 microscope using homemade software for the processing of micrographs.

RESULTS

Guinier patterns of the precipitate from acidified Na_2WO_4 solutions showed the identity of the product with crystalline tungstic acid, H_2WO_4, H_2O, compared and checked with the Joint Committee on Powder Diffraction Standards 1986 powder patterns, JCPDS 18–420. The product (Fig. 1) consists of thin cracked platelets ($\cong 5 \times 2 \times 0.2$ μm). On thermal dehydration the product loses 1 mole of water below 210°C and a second mole of water in a separate step below 325°C.

The sodium contents of the precipitates and the separated supernatant liquids from one preparation procedure are plotted in Fig. 2 versus the sequences of washing steps. The sodium content of the washed precipitate saturates at a level of 20–30 ppm after the seventh washing and centrifuging step, while the sodium content of the supernatant liquid decreases to 0.1 ppm, which is the level of sodium background for the used deionized water. Reproducibility limits and a comparison between Na analytical results using either NH_4OH or KOH for dissolution of the precipitate are demonstrated in Fig. 3, where sodium contents of the precipitates are plotted against the number of washing steps. The values of the sodium concentrations measured by using NH_4OH and KOH for dis-

FIG. 1. Scanning electron micrograph of precipitated tungstic acid, H_2WO_4, H_2O (JCPDF 18-420).

solution are close to each other and their behavior as the washing steps advanced is similar. Seven washing steps are needed to minimize the sodium concentration in H_2WO_4, H_2O at a level of 20 to 40 ppm.

The dehydration of H_2WO_4, H_2O with various residual or deliberately added sodium concentration in autoclave at 120°C resulted in the following. The products of the

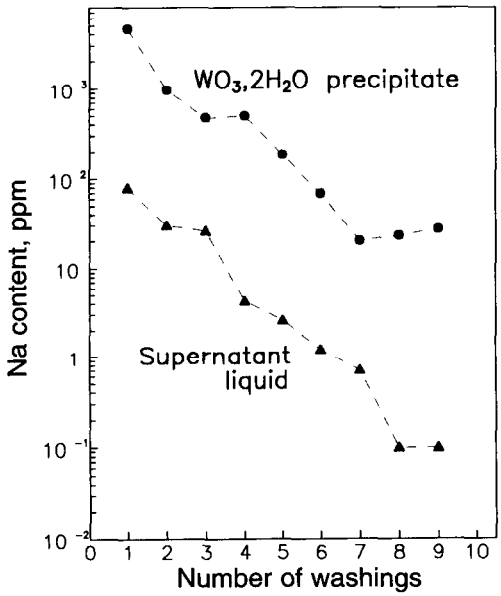

FIG. 2. Observed change in the sodium content in H_2WO_4, H_2O precipitate and in the rinsing liquid throughout the washing process (I.run). The sodium content of the washed precipitate saturates at a level of 20–30 ppm after the seventh washing and centrifuging step, while the sodium content of the supernatant liquid decreases to 0.1 ppm, which is the level of the sodium background of the used deionized water.

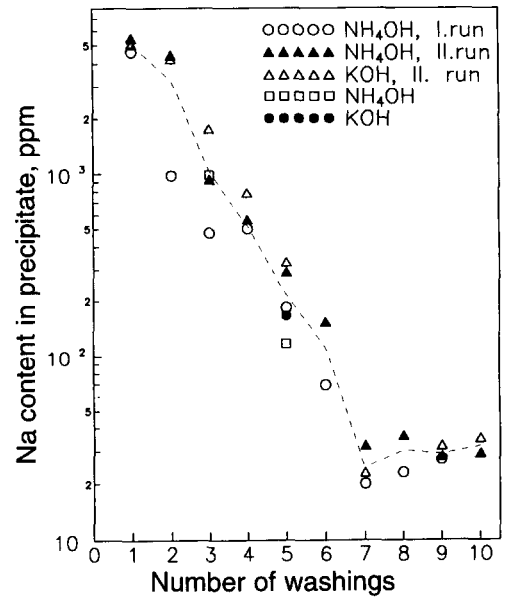

FIG. 3. Comparison of the sodium content data in H_2WO_4, H_2O precipitates at various washing runs using NH_4OH and KOH for dissolution of the precipitates.

dehydration consisted of either WO_3, $1/3H_2O$, JCPDS 35-270 or WO_3, H_2O, JCPDS 18-1418 crystals, or of a mixture of these two phases. WO_3, $1/3H_2O$ crystals formed in this autoclave process were all found to contain a minimum level (≅160 ppm) or above of sodium in the solid crystalline phase. If the obtained solid product contained sodium at a level as low as ≅40 ppm, instead of WO_3, $1/3H_2O$, the WO_3, H_2O phase crystallized in the same dehydration–crystallization process. An intermediate range of sodium concentration, with mixed growth of WO_3, $1/3H_2O$ and WO_3, H_2O phases, was also observed. Sodium concentration, color, structural characteristics, infrared transmittance peaks, and water loss at thermogravimetric measurements of the partially dehydrated samples from the autoclave are summarized in Table 1.

From the point of view of Na content of the solid phase, three ranges can be distinguished: Range I, no existence of WO_3, $1/3H_2O$, growth of WO_3, H_2O; Range II, mixed crystallite growth of WO_3, $1/3H_2O$ and WO_3, H_2O; and Range III, growth of WO_3, $1/3H_2O$. Lattice parameters of the orthorhombic WO_3, $1/3H_2O$ phases have been determined and are shown vs the Na content in Fig. 4. In the range of existence the lattice parameters *a* and *b* do not change, while parameter *c* seems to have a tendency to increase slightly. The shift of the 004 reflection with increasing sodium concentration compared to the 400 and 260 reflections is demonstrated in Fig. 5. In a sample of WO_3, $1/3H_2O$ with extremely high sodium concentration (3420 ppm) a splitting of the 400 diffraction peak (and of some other peaks, not shown in this figure) has been found.

TABLE 1
Summary of the Samples Prepared from H_2WO_4, H_2O

Sample	[Na] ppm	Color	Structure	H_2O equivalents per WO_3 groups (TG)	Infrared absorption wavenumber (cm^{-1}) assignation					
					δ_{W-O} (WO_6)	ν_{W-O-W} (WO_6)	ν_{W-O} (WO_6)	δ_{OH} (H_2O, OH)	νOH (H_2O)	ν_{OH} (W–OH)*
A13b/1	24	Yellow	WO_3, H_2O	0.70						
A5	41	Yellow	WO_3, H_2O	0.79	275	640	925	1610	3365	
					370		1070			
							1390			
A3	46	Yellow	WO_3, H_2O	0.63	285	650	925	1610	3370	
			$WO_3, 1/3H_2O$		370		1105			
						800	1400			
A10	54	Yellow	WO_3, H_2O	0.72	280	655	945	1606	3400	
			$WO_3, 1/3H_2O$		365	720				
					410	805				
A2	163	White	$WO_3, 1/3H_2O$	0.32	280	665	953	1604	3400	3480
					360	730	995			
					420	810				
A9	204	White	$WO_3, 1/3H_2O$	0.30	285	670	950	1602	3400	3480
					360	735	990			
					418	835				
A1	455	White	$WO_3, 1/3H_2O$	0.36	290	680	950	1601		3495
					360	740	995			
					422	815				
A4	495	White	$WO_3, 1/3H_2O$	0.40	290	680	965	1601		3495
					362	765	1010			
					424	820				
A14	605	White	$WO_3, 1/3H_2O$	0.43	290	680	955	1601		3495
					363	780	1000			
					426	820				
A6	740	White	$WO_3, 1/3H_2O$	0.39	290	670	950	1601		3495
					363	770	995			
					425	820				
A15	1053	White	$WO_3, 1/3H_2O$	0.43	280	675	950	1602		3497
					362	745	995			
					422	820				
A13b/2	3420	White	$WO_3, 1/3H_2O$	0.43	280	675	955	1605		3498
					364	730	1000			
					422	825				

Note. Samples prepared in autoclave at 120°C, 10 bar of $N_2 + O_2$ (80 : 20); stirring, 200 rpm, according to Ref. (4). The concentration of Na is determined by atomic absorption spectroscopy, the crystallographic structure by Guinier patterns, and the number of total H_2O equivalents per WO_3 groups contained in the samples from thermogravimetric measurements; for assignation of the infrared absorption bands see Refs. (15, 16, 17). A13b, two preparations of H_2WO_4, H_2O gels washed seven times were collected, homogenized, and parted into Samples A13b/1 and A13b/2. Before the sample was put into the autoclave, Na_2WO_4, $2H_2O$ was added (172 mg/2.33 g) to the H_2WO_4, H_2O gel of Sample A13b/2. WO_3, H_2O, JCPDS 18-1418; WO_3, $1/3H_2O$, JCPDS 35-270; W-OH*, attributed to the OH stretching vibration of W–OH ··· H_2O groups (17).

The crystal morphology of WO_3, $1/3H_2O$ crystallites is shown in Fig. 6. The octagonal platelets obtained from crystalline H_2WO_4, H_2O are similar to those reported in Ref. (4) and shown in Ref. (6). However, in Ref. (4) Furusawa's (14) and not Zocher's method was used for obtaining octagonal platelets of WO_3, $1/3H_2O$. The average linear dimension of the WO_3, $1/3H_2O$ crystallites was found to be dependent upon the sodium concentration detected in the solid phase (Fig. 7).

Infrared spectra of the products from the autoclave are shown in Figs. 8–10. The peaks of the ν(W–O–W) triplet (640–955 cm^{-1}), assigned to stretching vibration change with sodium concentration from the low concentration range to 160 ppm, scarcely change with higher concentrations (Fig. 8.), confirming the results of the X-ray investigations. The tendency of the changes of the deformation vibration peaks at lower frequencies (Fig. 9) is similar. The broad peak at about 1600 cm^{-1} (Fig. 8) assigned to

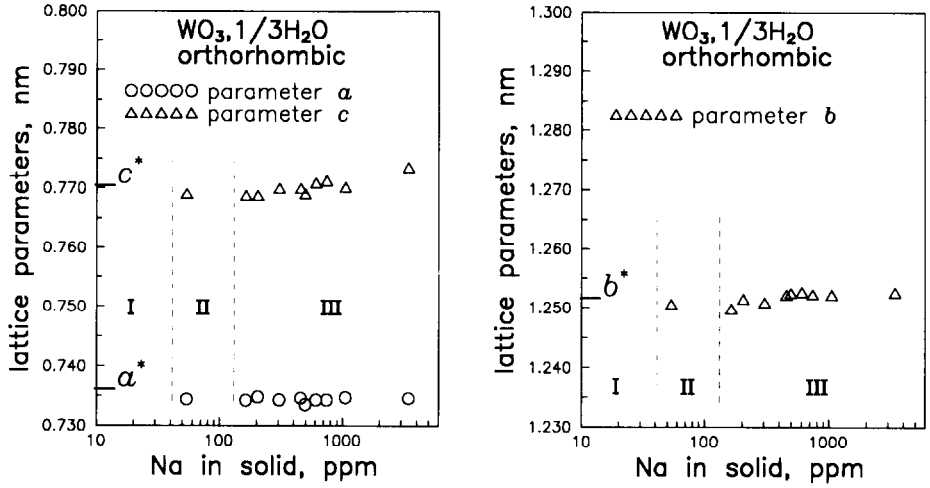

FIG. 4. Lattice parameters of the orthorhombic WO_3, $1/3H_2O$, JCPDS 35-270 samples containing various amounts of sodium. Ranges of the sodium content: Range I, [Na] < 46 ppm, no growth of WO_3, $1/3H_2O$; Range II, 46 < [Na] < 160 ppm, mixed growth of WO_3, H_2O, JCPDF 18-1418 and WO_3, $1/3H_2O$; Range III, [Na] > 160 ppm, growth of WO_3, $1/3H_2O$. a*, b*, and c* are lattice parameters from Ref. (4).

$\delta(OH)/H_2O/$ changes to a sharp peak of absorption at 160 ppm of sodium concentration that is associated with OH groups in W–OH. This change is connected with a decrease in the absorption wavenumber (Table 1). The $\nu(OH)/H_2O/$ transmittance plots are shown in Fig. 10. The broad band characteristic of OH groups associated with crystal water becomes narrower and shifts to higher frequencies with increasing sodium concentration. At 160 ppm of Na and at a wavenumber of 3480 cm^{-1}, $\nu(OH)$ of the OH group, associated with the W–OH ··· H_2O bonds (17) characteristic of WO_3, $1/3H_2O$ (4), dominates. The frequency of the $\nu(OH)$ peak continues to increase very slowly with sodium concentration (Table 1), while the peak itself changes remarkably, having a maximum at a sodium concentration of 740 ppm. From these spectra, we would say that spectrum *d* of Fig. 10, with [Na] = 163 ppm, and spectrum *f*, with [Na] = 455 ppm, seem to be similar to the spectra of octagonal platelets and needle aggregates of WO_3, $1/3H_2O$, respectively, reported in Fig. 5 of Ref. (4).

After subsequent heat treatments all theWO_3, $1/3H_2O$ samples with Na concentrations of 160 to 3400 ppm lost water and were transformed into the pseudomorphic metastable hexagonal WO_3 (Fig. 11), JCPDS 33-1387, at the same temperature as reported in Refs. (1 and 2).

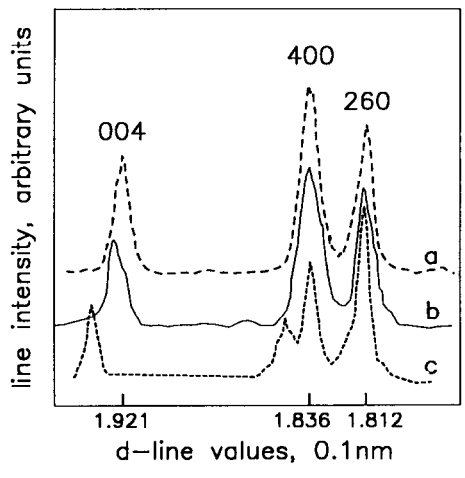

FIG. 5. X-ray powder diffraction patterns (densitometric analysis of the Guinier patterns) of WO_3, $1/3H_2O$ samples containing: a, 163; b, 1053; and c, 3420 ppm of sodium. The 400 and 260 reflections do not shift, while the 004 reflection shifts to the direction of the higher *d* lines. At the level of 3420 ppm sodium a split of the 400 reflection can be observed.

DISCUSSION

The most characteristic feature of this study is the fact that we have not succeeded in the preparation of WO_3, $1/3H_2O$ with a sodium content less than 160 ppm. However it was possible to control and analyze the sodium content of the precursor H_2WO_4, H_2O down to the level 20–30 ppm. Moreover, our impression is that sodium has an effective role either in controlling the reaction route of dehydration to the formation of WO_3, $1/3H_2O$, or in stabilizing the WO_3, $1/3H_2O$ phase.

Infrared and X-ray investigations indicate that the crystallographic structure of the WO_3, $1/3H_2O$ lattice (4) is not very sensitive to the presence of sodium in the range 160–3400 ppm. It is not clear at this point whether these limits can be considered exact values. Certainly, no variations in pressure, temperature, or processing time of the hydrothermal synthesis were made in this work.

The observation that the *c* parameter of the cell in-

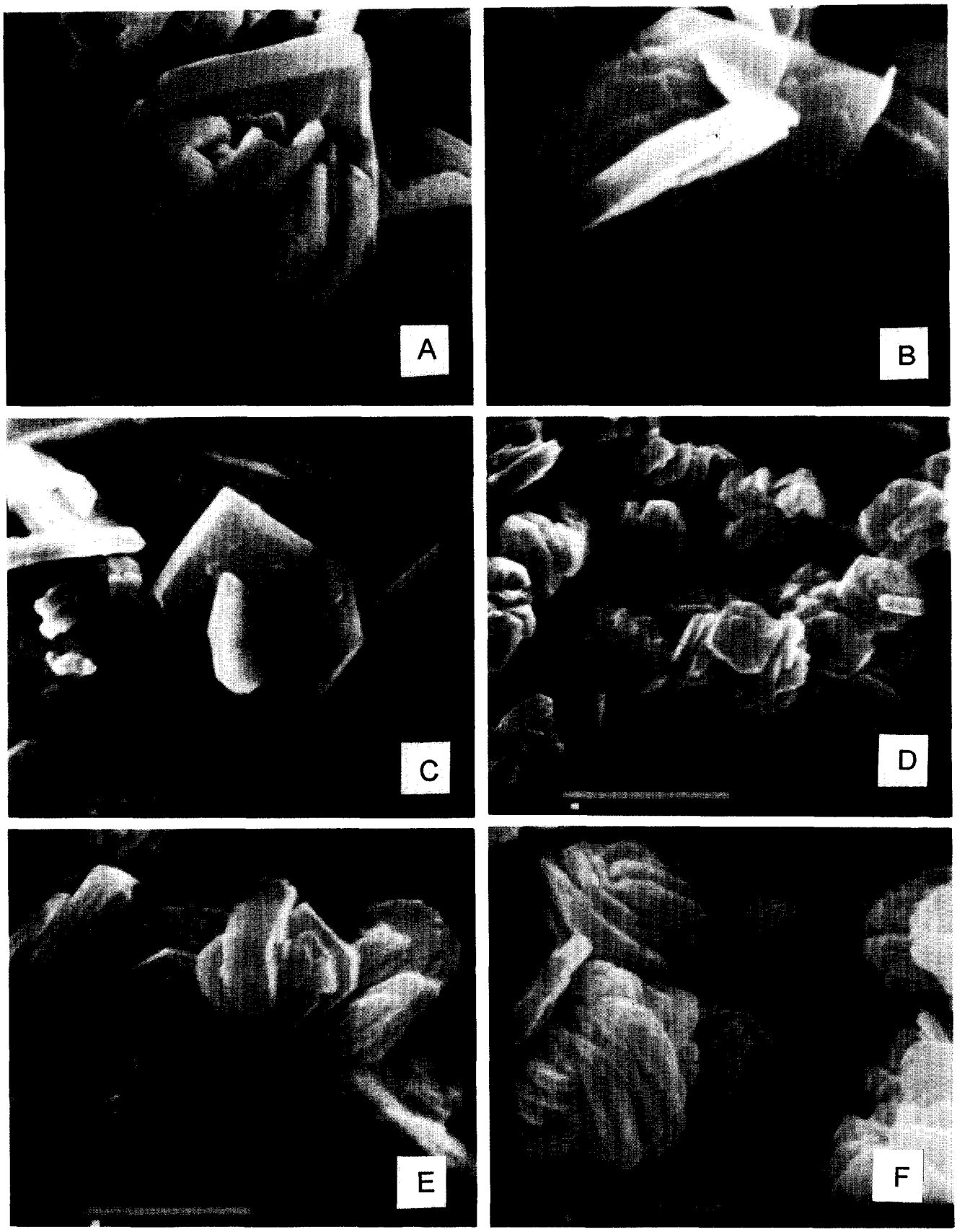

FIG. 6. Scanning electron micrographs of the orthorhombic WO_3, $1/3H_2O$, JCPDS 35-270 samples containing various amounts of sodium: A, 163; B, 204; C, 455; E, 740; D, 1053; and F, 3420 ppm.

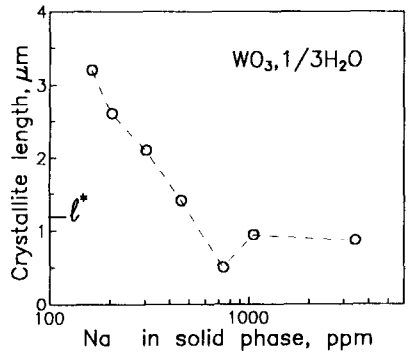

FIG. 7. The mean particle size of WO_3, $1/3H_2O$ crystallites vs their sodium content; l is the mean particle length from Ref. (4).

creases (the 004 reflection shifts) with the incorporation of sodium suggests that the role of a privileged facet during growth cannot be excluded. There is some evidence to indicate that a high level of incorporated sodium begins to deteriorate the WO_3, $1/3H_2O$ lattice. The observed incorporation raises the question of stoichiometry. The present results of chemical analysis indicate values of x from 0.00084 to 0.01786, using the formulation $(Na_2O)_xWO_3$, $1/3H_2O$. The significance of these values can be further emphasised using the reverse formulation Na_2O, $(WO_3, 1/3H_2O)_x$ with values of x from 56 to 1184. This formulation can be compared with "tungsten phase C," Na_2O, $(WO_3, 1/2H_2O)_{8\text{-}40}$ (18), JCPDS 17-616. The sodium content in "WO_3, $1/3H_2O$" is obviously much

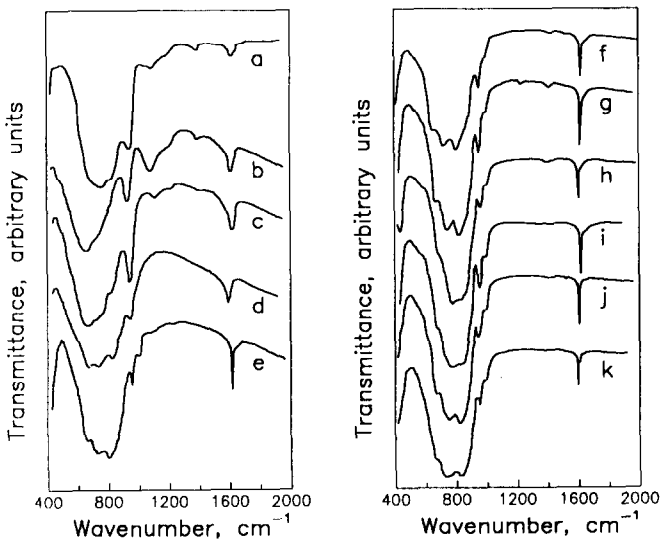

FIG. 8. Infrared spectra: a, WO_3, H_2O, [Na] = 11 ppm, from China National Nonferrous Metals Import & Export Corporation; b, WO_3, H_2O, [Na] = 41 ppm, from the autoclave; c and d, samples from the autoclave, mixed phases of WO_3, H_2O and WO_3, $1/3H_2O$, with [Na] = 46 and 54 ppm; e, f, g, h, i, j, and k, WO_3, $1/3H_2O$ samples from the autoclave, with [Na] = 163, 204, 455, 605, 740, 1053, and 3420 ppm.

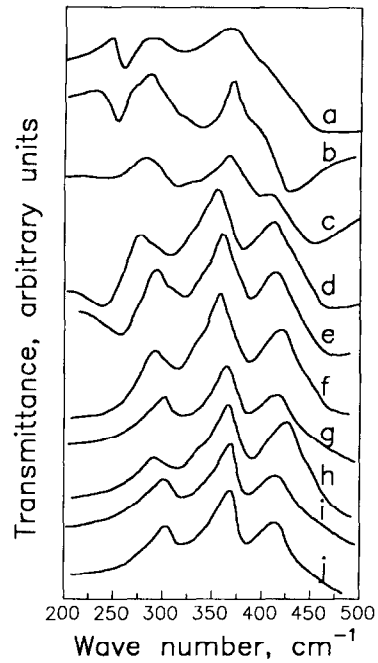

FIG. 9. Infrared spectra: a, WO_3, H_2O, [Na] = 11 ppm, from China National Nonferrous Metals Import & Export Corporation; b, WO_3, H_2O, [Na] = 41 ppm, from the autoclave; c, mixed phases of WO_3, H_2O and WO_3, $1/3H_2O$ from the autoclave, [Na] = 54 ppm; d, e, f, g, h, i, and j, WO_3, $1/3H_2O$ samples from the autoclave, with [Na] = 163, 204, 455, 605, 740, 1053, and 3420 ppm.

smaller than in phase C, and little can be said about the way of incorporation—whether Na is adsorbed on certain facets or whether it occupies defect sites in the lattice. NMR studies (10) have shown that 3% of the protons in octagonal platelets of WO_3, $1/3H_2O$ belong to OH groups, and it has been assumed that these OH groups are located on the surface of the crystallites. The range of sodium content of our WO_3, $1/3H_2O$ samples is in agreement with the concentration of the OH groups determined in Ref. (10). This agreement seems to make the idea of locating sodium on crystal facets somewhat possible. On the other hand, however, the observed shift of the 004 reflections indicate sodium incorporation into the cell.

Interpreting our experimental results, we would stress that all the procedures were performed according to the detailed report in Ref. (4), therefore we have reason to suppose that samples of that study also contained a not-negligible level of sodium.

The observation of the sodium content (or contamination) of WO_3, $1/3H_2O$ samples discussed here can have other consequences. If sodium is present in the WO_3, $1/3H_2O$ phase, the dehydration product, h-WO_3, will contain sodium as well. This raises the question of the stoichiometry of the metastable h-WO_3. This very important question is being studied now and the results will be published later.

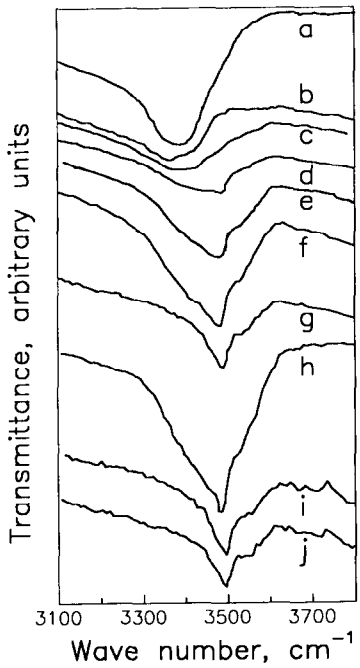

FIG. 10. Infrared spectra: a, WO_3, H_2O, [Na] = 11 ppm, from China National Nonferrous Metals Import & Export Corporation, b, WO_3, H_2O, [Na] = 41 ppm, from the autoclave; c, mixed phases of WO_3, H_2O and WO_3, $1/3H_2O$ from the autoclave, [Na] = 54 ppm; d, e, f, g, h, i, and j, WO_3, $1/3H_2O$ samples from the autoclave with [Na] = 163, 204, 455, 605, 740, 1053, and 3420 ppm.

SUMMARY AND CONCLUSION

Reproducing the preparation route of WO_3, $1/3H_2O$ reported in Ref. (4), the same phase (within experimental error, with the same lattice parameters) of the same color and crystallite shape was grown. During subsequent heat treatments the samples lost water and were transformed into the pseudomorphic metastable hexagonal WO_3, as reported in Refs. (1 and 2). All WO_3, $1/3H_2O$ samples have been found to contain sodium (160–1100 ppm). Using precursors with a low (20–30 ppm) level of sodium instead of WO_3, $1/3H_2O$, the formation of WO_3, H_2O has been observed. After a deliberate Na addition WO_3, $1/3H_2O$ was obtained again from the same precursor. X-ray powder diffraction and infrared absorption measurements have been used to confirm that sodium incorporates into the WO_3, $1/3H_2O$ phase, stabilizing it and changing its stoichiometry to Na_2O, $(WO_3, 1/3H_2O)_x$ with values of x from 56 to 1184.

FIG. 11. SEM micrograph of the hexagonal WO_3 obtained by isotherm dehydration at 290°C of WO_3, $1/3H_2O$ with [Na] = 455 ppm.

ACKNOWLEDGMENTS

We thank Professor L. Bartha for his support in this work, Dr. G. Gerey for his collaboration in the preparation of the samples, and Mr. A. Tóth for SEM photographs. We also thank Dr. P. Arató, Mr. F. Wéber, and Mr. S. Gurbán for helpful discussions.

REFERENCES

1. B. Gerand, G. Nowogrocki, J. Guenot, and M. Figlarz, *J. Solid State Chem.* **29,** 429–434 (1979).
2. M. Figlarz and B. Gerand, *in* "9th International Symposium on the Reactivity of Solids, Cracow, Poland," (K. Dyreh, J. Haber, and J. Nowotny, Eds.), pp. 887–891. Elsevier, Amsterdam, 1980.
3. K. H. Cheng, A. J. Jacobson, and M. S. Whittingham, *Solid State Ionics* **5,** 355–358, (1981).
4. B. Gerand, G. Nowogrocki, and M. Figlarz, *J. Solid State Chem.* **38,** 312–320 (1981).
5. B. Vidick, J. Lemaitre, and B. Delmon, *Acta Chim. Hung.* **111,** 449–463 (1982).
6. M. Figlarz, B. Dumont, B. Gerand, and B. Beaudoin, *J. Microsc. Spectrosc. Electron.* **7,** 371–386, (1982); M. Figlarz, *Prog. Solid State Chem.* **19,** 1–46 (1989).
7. B. Gerand and M. Figlarz, "Reduction of Hexagonal WO_3 by Hydrogen Spillover: Formation of New Hydrogen Hexagonal Tungsten Bronzes H_xWO_3 in Spillover of Adsorbed Species," (G. M. Pajonk, S. J. Teichner, and J. E. Germain, Eds.). Elsevier, Amsterdam, 1983.
8. S. Laurelle and M. Figlarz, *J. Solid State Chem.* **111,** 172–179 (1994).
9. J. C. Newton-Hoves and A. N. Cormack, *J. Solid State Chem.* **79,** 12–18 (1989).
10. C. Doremieux-Morin, L. G. de Menorval, and B. Gerand, *J. Solid State Chem.* **45,** 193–199 (1982).
11. H. Zocher and K. Jacobson, *Kolloidchem. Beih.* **28,**(6), 167 (1929).
12. G. M. Neumann, *Talanta* **18,** 1047–1057 (1971).
13. Installed by L. Petrás and L. Nagy, unpublished.
14. K. Furusawa and S. Hachisu, *Sci. Light (Tokyo)* **15,** 115–130 (1966).
15. A. B. Kiss, *Acta Chim Acad. Sci. Hung.* **75,** 351–368 (1973).
16. A. B. Kiss, *Acta Chim Acad. Sci. Hung.* **84,** 393–407 (1975).
17. M. F. Daniel, B. Desbat, J. C. Lassegues, B. Gerand, and M. Figlarz, *J. Solid State Chem.* **67,** 235–247 (1987).
18. M. L. Freedman and S. Leber, *J. Less-Common Met.* **7,** 427–432 (1964).